Dual Inhibition of Human Type 4 Phosphodiesterase Isostates by (*R**,*R**)-(±)-Methyl 3-Acetyl-4-[3-(cyclopentyloxy)-4-methoxyphenyl]-3-methyl-1-pyrrolidinecarboxylate

Gaochao Tian,*[,‡] Warren J. Rocque,[§] Jeffrey S. Wiseman,[||,▽] Irene Z. Thompson,[‡,○] William D. Holmes,[§] Paul L. Domanico,[||] Jeffrey A. Stafford,[⊥] Paul L. Feldman,[⊥] and Michael A. Luther[§]

Departments of Molecular Biochemistry, Molecular Sciences, and Medicinal Chemistry and Division of Research Information Resources, Glaxo Wellcome Inc., Research Triangle Park, North Carolina 27709

Received October 30, 1997

ABSTRACT: Purified recombinant human type 4 phosphodiesterase B2B (HSPDE4B2B) exists in both a low- and a high-affinity state that bind (*R*)-rolipram with K_d's of ca. 500 and 1 nM, respectively [Rocque, W. J., Tian, G., Wiseman, J. S., Holmes, W. D., Thompson, I. Z., Willard, D. H., Patel, I. R., Wisely, G. B., Clay, W. C., Kadwell, S. H., Hoffman, C. R., and Luther, M. A. (1997) *Biochemistry 36*, 14250−14261]. Since the tissue distribution of the two isostates may be significantly different, development of inhibitors that effectively inhibit both forms may be advantageous pharmacologically. In this study, enzyme inhibition and binding of HSPDE4B2B by (*R**,*R**)-(±)-methyl 3-acetyl-4-[3-(cyclopentyloxy)-4-methoxyphenyl]-3-methyl-1-pyrrolidinecarboxylate (**1**), a novel inhibitor of phosphodiesterase 4 (PDE 4), were investigated. Binding experiments demonstrated high-affinity binding of **1** to HSPDE4B2B with a stoichiometry of 1:1. Inhibition of PDE activity showed only a single transition with an observed K_i similar to the apparent K_d determined by the binding experiments. Deletional mutants of HSPDE4B2B, which have been shown to bind (*R*)-rolipram with low affinity, were shown to interact with **1** with high affinity, indistinguishable from the results obtained with the full-length enzyme. Bound **1** was completely displaced by (*R*)-rolipram, and the displacement showed a biphasic transition that resembles the biphasic inhibition of HSPDE4B2B by (*R*)-rolipram. Theoretical analysis of the two transitions exemplified in the interaction of (*R*)-rolipram with HSPDE4B2B indicated that the two isostates were nonexchangeable. Phosphorylation at serines 487 and 489 on HSPDE4B2B had no effect on the stoichiometry of binding, the affinity for binding, or the inhibition of the enzyme by **1**. These data further illustrate the presence of two isostates in PDE 4 as shown previously for (*R*)-rolipram binding and inhibition. In contrast to (*R*)-rolipram, where only one of the two isostates of PDE 4 binds with high affinity, **1** is a potent, dual inhibitor of both of the isostates of PDE 4. Kinetic and thermodynamic models describing the interactions between the nonexchangeable isostates of PDE 4 and its ligands are discussed.

Phosphodiesterases (PDEs)[1] comprise a large, divergent family of enzymes that catalyze hydrolysis of the second messengers cAMP and cGMP to produce a 5′-nucleoside monophosphate. The enzymes in this family can be categorized into at least seven types, which differ in their kinetic properties, substrate selectivity, response to activators and inhibitors, primary sequences, etc. (*1*−*3*). Dependent upon the type and tissue distribution, altered activity of PDE has been implicated in a number of biological disorders, including retinal degeneration (*4*, *5*), congestive heart failure (*6*, *7*), asthma (*8*, *9*), and inflammation (*11*, *12*). Therefore, type- or tissue-specific inhibitors of PDE are of great interest pharmacologically.

From early studies, (*R*)-rolipram (Figure 1), a type 4 PDE-specific inhibitor, was reported to bind the enzyme with a $K_d \sim 1$ nM (*13*, *14*) but only to inhibit the enzyme with an affinity that is 1000-fold less ($K_i \sim 1$ μM) (*15*). As a result, type 4 PDE was thought to have two sites for (*R*)-rolipram binding with different catalytic and binding characteristics. Because the inhibition appeared to be competitive versus substrate (*15*), the "low-affinity site" was proposed to be an enzyme active site. Coexpression of both human type 4 PDE activity and high-affinity (*R*)-rolipram binding in yeast suggested the presence of the "high-affinity site" on the same

[‡] Department of Molecular Biochemistry.
[§] Department of Molecular Sciences.
[||] Division of Research Information Resources.
[▽] Current address: Research Computing, Smith Kline Beecham Pharmaceuticals, 709 Swedeland Rd., POB 1539, King of Prussia, PA 19406-0939.
[○] Current address: Markey Center for Cell Signaling, the University of Virginia Medical Center, Charlottesville, VA 22908.
[⊥] Department of Medicinal Chemistry.
* To whom correspondence should be addressed. Telephone: (919) 483-5678. Fax: (919) 483-4320. E-mail: GT14994@glaxo.com.

[1] Abbreviations: BSA, bovine serum albumin; cAMP, adenosine 3′,5′-cyclic monophosphate; cGMP, guanosine 3′,5′-cyclic monophosphate; DMSO, dimethyl sulfoxide; DTT, *dl*-dithiothreitol; EDTA, ethylenediaminetetraacetic acid; HEPES, *N*-(2-hydroxyethyl)piperazine-*N*′-2-ethanesulfonic acid; HSPDE4B2B, human recombinant phosphodiesterase 4 isoform B; MAPK, mitogen-activated protein kinase; PDE, phosphodiesterase; PEI, polyethylenimine; Tris, tris(hydroxymethyl)aminomethane; **1**, (*R**,*R**)-(±)-methyl 3-acetyl-4-[3-(cyclopentyloxy)-4-methoxyphenyl]-3-methyl-1-pyrrolidinecarboxylate.

S0006-2960(97)02700-1 CCC: $15.00
Published on Web 04/23/1998

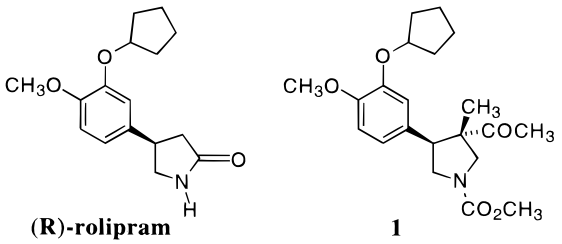

FIGURE 1: Chemical structures of (*R*)-rolipram and (*R**,*R**)-(±)-methyl 3-acetyl-4-[3-(cyclopentyloxy)-4-methoxyphenyl]-3-methyl-1-pyrrolidinecarboxylate (**1**).

enzyme molecule (*16*). However, high-affinity binding was not shown previously in any inhibition studies, and therefore, this site was thought to be noncatalytic. Its location in the primary structure and the functional relationship with the low-affinity site remained elusive and puzzling. The availability of purified human PDE 4 B2B (HSPDE4B2B) in milligram quantities (*17*, *18*) prompted us to reevaluate the mechanism of (*R*)-rolipram binding of PDE 4 (*19*). Analysis of progress curves for the HSPDE4B2B reaction in the presence of (*R*)-rolipram indicated time-dependent inhibition (*19*). Subsequent preincubation of enzyme with (*R*)-rolipram revealed a biphasic inhibition curve displaying a previously unseen nanomolar K_i, indicative of a catalytic function for the high-affinity site (*19*). Filter binding, equilibrium dialysis, and microcalorimetry confirmed a stoichiometry of no more than 1:1 for (*R*)-rolipram binding (*19*). These data unambiguously demonstrated the existence of one site, but two states, of HSPDE4B2B that are both catalytically active. Data from examining truncational mutants indicated that the N-terminal amino acid residues of HSPDE4B2B are important in determining the high-affinity state. (*R*)-Rolipram, although it is type 4 PDE-specific, is a poor inhibitor for the low-affinity state of the enzyme.

It is intriguing if the expression of the two isostates of HSPDE4B2B is restricted to (*R*)-rolipram binding and, if not, whether these states will display the same type of kinetic and thermodynamic properties in their interactions with other inhibitors. In this study, we describe a novel compound, (*R**,*R**)-(±)-methyl 3-acetyl-4-[3-(cyclopentyloxy)-4-methoxyphenyl]-3-methyl-1-pyrrolidinecarboxylate (**1**, Figure 1), that binds and inhibits both states of HSPDE4B2B with high affinity.

EXPERIMENTAL PROCEDURES

Materials. (*R*)-Rolipram and **1** were synthesized as described (*20*). [^{3}H]**1** (82 Ci/mmol) was prepared by Dr. Shimoga Prakash (Glaxo Wellcome Research Institute, Research Triangle Park, NC). Ninety-six-well microtiter plates were from Costar; 96-well micro β scintillation plates and Optiphase High Safe 3 scintillation fluid were from Wallac; and the microdialyzer and equilibrium dialysis membranes were from Hoeffer Scientific. Nucleotidase and all other chemicals were of the highest grade from Sigma.

Expression, Mutation, and Purification of HSPDE4B2B Constructs. HSPDE4B2B constructs 1−564, 81−564, and 81−564 with serine to alanine mutations at residues 482, 487, and 489 (81−564 SΔA), and 152−528 and 152−528 with serine to alanine mutations at residues 482, 487, and 489 (152−528 SΔA) were expressed and purified as previously described (*17*−*19*).

Protein Concentration Determination. Protein concentrations were determined both by a modified Bradford analysis (BioRad) and by quantitative amino acid analysis. Gas-phase hydrolysis with 6 N HCl was carried out for 1 h at 150 °C. Free amino acids were analyzed using an Applied Biosystems 420A derivatizer with a 130A separation system and a 920A data analysis module. Insulin was used as a calibration standard in the same buffer as HSPDE4B2B.

PDE Activity Assays. All PDE enzyme activity assays were performed at 22 °C, pH 7.5, as described previously (*19*).

Inhibition Kinetics. Compound **1** was prepared in 10% DMSO and added to the reaction mixture for assaying PDE enzyme activity with 10× dilution such that the final DMSO concentration was maintained at 1%. The concentration of cAMP was kept at much less than its K_m throughout the inhibition studies. Thus the pseudo first-order rate constant (V/K) was calculated as $-\ln([S]/S_t)/\Delta t$, where S is substrate; S_t, the total concentration of substrate; and Δt, the reaction time. The kinetic inhibition data were fit to

$$R \equiv 1 - \frac{V/K + b}{(V/K)_0} = \frac{[I]}{K_i + [I]} \qquad (1)$$

where $(V/K)_0$ is enzyme activity in the absence inhibitor, [I] is the concentration of inhibitor, and K_i is the inhibition constant. The constant b represents the background due to flow-through of radioactivity during the filtration step in the absence of enzyme.

Filter Binding Assays. All filter binding assays were conducted in 2 mM Tris-HCl, pH 7.5, containing 0.2 mM DTT, 0.2 mM EDTA, 1 mM $MgCl_2$, and 0.5 mg/mL BSA. Glass fiber filter mats were pretreated with 0.3% PEI for 2 h and dried before use. Solutions containing [^{3}H]**1** and HSPDE4B2B at specified concentrations were prepared in 96-well plates. The mixtures were incubated at room temperature (22 °C) for 1 h and cooled for 15 min at 4 °C before filtration. All of the subsequent steps were performed at 4 °C. The binding mixtures were filtered through a PEI-treated glass fiber filter mat in a Tomtec cell harvester by an automated sequence of aspiration and washing. A 5-s aspiration trapped the enzyme−ligand complex on the filter mat. The free ligand was removed immediately by a 3.5-s (unless specified otherwise) wash with 25 mM Tris-HCl, pH 7.4, containing 100 mM NaCl. The filter was dried for 15 s with house vacuum attached to the harvester and further dried to complete dryness in air in a hood at room temperature. The dried filter mat was placed between two sheets of Meltilex solid scintillant in a plastic scintillation bag. This was heated on a hot plate at 80 °C until the scintillant was uniformly soaked into the filter mat. The scintillation bag was heat-sealed, placed in a cassette, and counted for tritium in a Wallac 1450 micro β scintillation counter. The counts were converted to molar concentration of bound ligand after correction for counting and capturing efficiencies.

*Determination of Off-Rates for Dissociation of **1** from the **1**-HSPDE4B2B Complex.* The filter binding assay procedure was used to determine off-rates of **1** from **1**−HSPDE4B2B. Solutions containing [^{3}H]**1** (2 nM) and HSPDE4B2B 1−564 (1 nM) were prepared in 96-well plates. The concentrations of enzyme−ligand complex in these solutions were deter-

Scheme 1: Inhibitor Binding to a Two State Enzyme System[a]

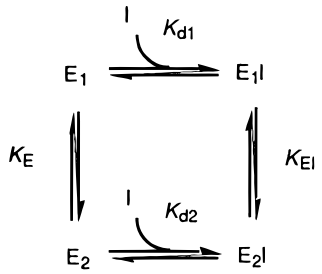

[a] I is inhibitor, E_1 and E_2 are the isostates 1 and 2 of enzyme, respectively, K_{d1} and K_{d2} are dissociation constants for E_1I and E_2I, respectively; and K_E and K_{EI} are the equilibrium constants for the equilibria between E_2 and E_1 and between E_2I and E_1I, respectively.

mined by the filter binding procedure (see Filter Binding Assays) using different washing times. Triplicates were performed for each time point. The data were analyzed according to a first-order decay to obtain the off-rate constant, k_{off}.

Determination of K_d by Filter Binding Assay. HSPDE4B2B 1−564 at a fixed concentration of 1 nM was mixed with various concentrations of [^{3}H]**1** in a 96-well plate. After incubation at room temperature for 1 h, the plate was chilled at 4 °C for 15 min. The inhibitor−enzyme complex was trapped and quantitated by using the filter binding assay procedure described above. The dissociation constant, K_d, was determined by fitting the data to

$$[EI] = {}^1/_2(E_t + I_t + K_d - \sqrt{(E_t + I_t + K_d)^2 - 4E_tI_t}) \quad (2)$$

where [EI] represents the concentration of enzyme−inhibitor complex and E_t and I_t are the total concentrations of enzyme and inhibitor, respectively.

Thermodynamic Equations for a Two-State System. The thermodynamic system for a two-state binding reaction is depicted in Scheme 1. The dissociation constants K_{d1} and K_{d2} and the equilibrium constants K_E and K_{EI} are defined, respectively, as

$$K_{d1} = \frac{[E_1][I]}{[E_1I]} \quad (3)$$

$$K_{d2} = \frac{[E_2][I]}{[E_2I]} \quad (4)$$

$$K_E = \frac{[E_1]}{[E_2]} \quad (5)$$

and

$$K_{EI} = \frac{[E_1I]}{[E_2I]} \quad (6)$$

where the subscripts 1 and 2 represents the states 1 and 2, respectively. The mass balances are given by

$$E_t = [E_1] + [E_2] + [E_1I] + [E_2I] \quad (7)$$

and

$$I_t = [I] + [E_1I] + [E_2I] \quad (8)$$

where I_t and [I] are total and free inhibitor concentrations, respectively. Assuming $I_t \gg E_t$, I_t can be approximated by [I]. Using eqs 3−8, it can be demonstrated that the equilibrium concentrations of enzyme−inhibitor species are given by (Appendix A):

$$[E_1I] = E_t\frac{A_1[I]}{(K_{d1})_{app} + [I]} \quad (9)$$

where

$$A_1 = \frac{1}{1 + \frac{1}{K_{EI}}} \quad (10)$$

and

$$(K_{d1})_{app} = K_{EI}\frac{1 + K_E}{1 + K_{EI}}K_{d1} \quad (11)$$

and

$$[E_2I] = E_t\frac{A_2[I]}{(K_{d2})_{app} + [I]} \quad (12)$$

where

$$A_2 = \frac{1}{1 + K_{EI}} \quad (13)$$

and

$$(K_{d2})_{app} = K_E\frac{1 + K_E}{1 + K_{EI}}K_{d2} \quad (14)$$

If E_1 and E_2 are not exchangeable, eqs 9 and 12 can be reduced, respectively, to

$$[E_1I] = E_{1t}\frac{[I]}{K_{d1} + [I]} \quad (15)$$

and

$$[E_2I] = E_{2t}\frac{[I]}{K_{d2} + [I]} \quad (16)$$

where E_{1t} and E_{2t} are total concentrations of E_1 and E_2.

*Filter Binding Displacement of **1** by (R)-Rolipram.* Solutions containing [^{3}H]**1** at 2 nM and a HSPDE4B2B construct at 1 nM were prepared as for filter binding assays. (*R*)-Rolipram at various concentrations was included in the mixture. The concentration of bound [^{3}H]**1** was determined as described in Filter Binding Assays. The data were fit either to a one-state model or to a model of two nonexchangeable states, respectively, according to (see Results)

$$[EI_h] = \frac{[EI_h]_{[I_c]=0}}{1 + \frac{[I_c]}{(IC_{50})}} + b \quad (17)$$

and

$$[EI_h] = \frac{[E_1I_h]_{[I_c]=0}}{1 + \frac{[I_c]}{(IC_{50})_1}} + \frac{[E_2I_h]_{[I_c]=0}}{1 + \frac{[I_c]}{(IC_{50})_2}} + b \qquad (18)$$

where the subscripts h and c represent radiolabeled **1** and cold (*R*)-rolipram, respectively, and the IC_{50} values for states 1 or 2 are given by

$$IC_{50} = K_{dc}\left(1 + \frac{[I_h]}{K_{dh}}\right) \qquad (19)$$

where K_{dc} and K_{dh} represent the dissociation constants for the cold and hot inhibitors, respectively.

Job Plot Assays. Job plot filter binding assays of HSPDE4B2B−inhibitor binding were performed according to published procedures (*19*) with minor modifications. A solution of [^{3}H]**1** estimated at 100 nM was prepared in the Tris buffer (see Filter Binding Assays) containing 1% DMSO. The actual concentration of **1** was then determined by measuring the radioactivity of the solution against a tritium standard and by using the known specific activity (82 Ci/mmol) of [^{3}H]**1**. The stock solutions of different constructs of HSPDE4B2B were prepared at the same concentration as the [^{3}H]**1** solution. Solutions of [^{3}H]**1** and enzyme at various molar fractions of enzyme but at a constant sum of enzyme and ligand were prepared in a 96-well plate. Concentrations of enzyme−ligand complex, [EI], of the solutions were determined according to the procedure described in Filter Binding Assays and plotted against the molar fraction of enzyme, χ_e. The data corresponding to χ_e values of 0−0.3 (data set 1) and 0.7−1.0 (data set 2) were fit to the following linear functions, respectively,

$$[EI] = s_1\chi_e \qquad (20)$$

and

$$[EI] = i_2 - s_2\chi_e \qquad (21)$$

where s_1 and s_2 are the slopes for data sets 1 and 2, respectively, and i_2 is the intercept of the *y* axis for data set 2. The values of molar fraction that correspond to the [EI] value at the intercept of the two lines, $(\chi_e)_s$, is given by

$$(\chi_e)_s = \frac{i_2}{s_1 + s_2} \qquad (22)$$

The stoichiometry of the binding, *n*, is calculated by (*21*, *22*)

$$n = \frac{1 - (\chi_e)_s}{(\chi_e)_s} \equiv \frac{s_1 + s_2}{i_2} - 1 \qquad (23)$$

The K_d for a binding reaction with 1:1 stoichiometry can be obtained by fitting the data to (Appendix B)

$$[EI] = {}^1/_2(C_t + K_d - \sqrt{(C_t + K_d)^2 - 4C_t{}^2(\chi_e - \chi_e{}^2)} \qquad (24)$$

where C_t is the sum of the total concentrations of enzyme and ligand.

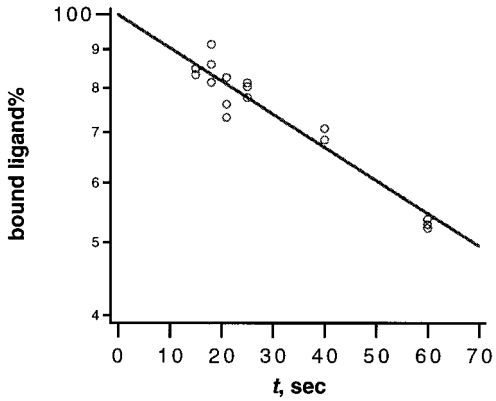

FIGURE 2: Time course of release of the [^{3}H]**1**−HSPDE4B2B complex from a glass fiber filter mat. [^{3}H]**1** (2 nM) and HSPDE4B2B (1 nM) were mixed and incubated at 22 °C for 1 h, followed by a 15-min chill on ice. The mixture was filtered at 4 °C through a PEI-treated glass fiber filter mat. The **1**−HSPDE4B2B complex trapped on the filter mat was washed with 100 mM NaCl for various durations. The bound ligand was then quantitated by ^{3}H counts.

Equilibrium dialysis Job plot assays were performed for binding reactions of **1** and HSPDE4B2B 81−564 SΔA or 152−528 SΔA mutants using a Hoeffer microdialyzer. The protein stock solutions, in 50 mM HEPES, pH 7.5, 150 mM NaCl, 2.5 mM $MgCl_2$, and 0.5% DMSO, were prepared at the same concentration (2 μM) as [^{3}H]**1**. The [^{3}H]**1** and enzyme, with various molar fractions but at a constant sum of enzyme and ligand, were added to one side of an equilibrium dialysis chamber. An equal volume of 50 mM HEPES, pH 7.5, 150 mM NaCl, 2.5 mM $MgCl_2$, and 0.5% DMSO was added to the other side. The chambers were separated by a 12−14 kDa molecular weight cutoff membrane. The enzyme−inhibitor solution was dialyzed at 4 °C for 20 h. Fifty microliters of sample from the HSPDE4B2B−inhibitor side (bound + free ligand) and the same volume from the side without protein (free ligand) were pipetted into separate wells of a 96-well micro β scintillation plate. After addition of 200 μL of Optiphase High Safe 3 liquid scintillant, the plates were counted in the same counter as above. The bound counts (cpm), [(bound + free) − (free)], were plotted against the molar fraction of enzyme, χ_e, and the stoichiometry derived from eq 23.

RESULTS

*Compound **1** Binds and Inhibits Full-Length HSPDE4B2B with High Affinity*. Filter binding assays were used to examine the affinity of **1** for purified full-length (1−564) recombinant HSPDE4B2B. After the enzyme−ligand complex was trapped on PEI-treated fiberglass filter mats, free ligand was routinely removed by a 3.5-s buffer wash. To assess whether the ligand that was bound with enzyme might also have been washed off the filter, a time course of radioligand remaining versus wash time was monitored. As shown in Figure 2, the counting rate decays as the wash time increases, but it does with a relatively long half-life ($t_{1/2}$ = 69 s) compared to the duration of the wash (3.5 s). Therefore, although principally a nonequilibrium method, the filter binding procedure captured equilibrium concentrations of bound ligand under the conditions used.

Nonspecific binding to filter mats became noticeable as the total amount of radioligand increased. The amount of

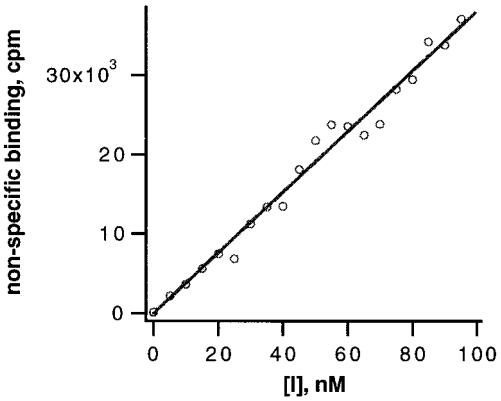

FIGURE 3: Correlation between the nonspecific binding of **1** on PEI-treated glass fiber filter mats and the concentration of **1**. [^{3}H]-**1** was prepared at different concentrations and filtered though a PEI-treated glass fiber filter mat. This was then followed by a 3.5-s, 100 mM NaCl wash. Nonspecific binding was quantitated by counting ^{3}H associated with the mat.

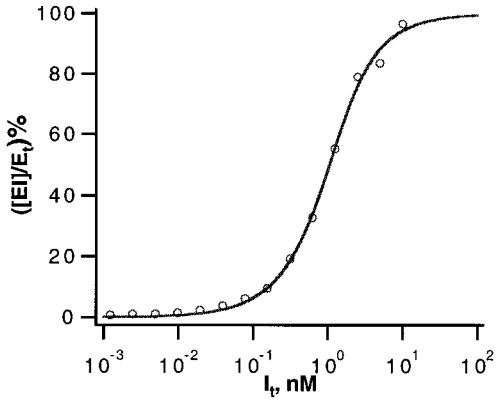

FIGURE 4: Percent of **1**−HSPDE4B2B complex ([EI]/E_t) as a function of the total concentration of ligand, I_t, determined by direct filter binding experiments. The enzyme concentration was set to 1 nM for each value of I_t. The mixtures prepared in a 96-well plate were incubated at room temperature (22 °C) for 1 h and then filtered through a PEI-treated glass fiber filter mat. After the filter mat was washed with 100 mM NaCl for 3.5 s, the values of radioactivity that correspond to different values of I_t were measured in a micro β counter. Data were fit to eq 2.

nonspecific binding as a function of the radioligand concentration was monitored. As shown in Figure 3, the nonspecific binding was linear with the concentration of radioligand with a slope of 381 cpm/nM. In subsequent experiments, nonspecific binding, either estimated using the linear relationship or determined in a parallel control, was subtracted from total binding.

Titration of radiolabeled **1** against a constant concentration (1 nM) of full-length HSPDE4B2B is best described by an apparent single binding transition (Figure 4) with a K_d of 0.55 ± 0.05 nM, a value that resembles that for the high-affinity state for (*R*)-rolipram. However, if present, a low-affinity binding transition might have escaped detection by the filter binding assays. To evaluate this possibility, we turned to inhibition studies. The inhibition curve (Figure 5A) again reveals only a single transition with a K_i of 0.54 ± 0.10 nM (Table 1), a value that is indistinguishable from the K_d determined by the filter binding method. This is in contrast with the results obtained for (*R*)-rolipram where data clearly indicate two forms of enzyme with a several 100-

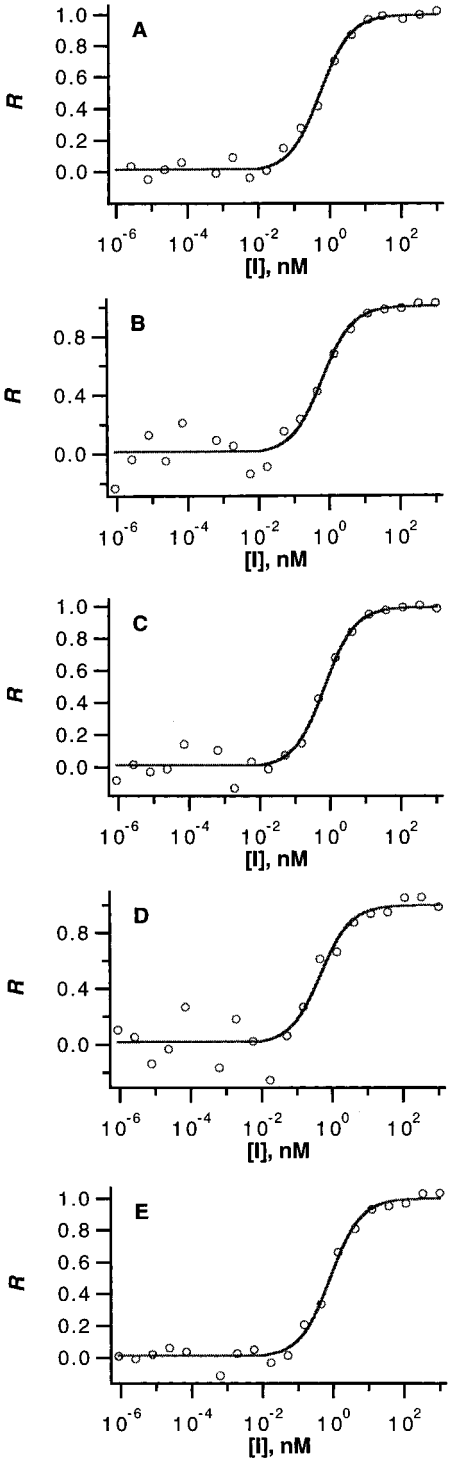

FIGURE 5: Inhibition of HSPDE4B2B constructs and site-specific mutants by **1**. The enzyme assays were carried out as described in Experimental Procedures. The activity data at different [I] values were analyzed according to the model of competitive inhibition, and the results were plotted as the degree of inhibition, *R* (eq 1), vs [I]. (A) HSPDE4B2B 1−564. (B) HSPDE4B2B 81−564. (C) HSPDE4B2B 152−528. (D) HSPDE4B2B 81−564 SΔA. (E) HSPDE4B2B 152−528 SΔA.

fold difference in affinity for the inhibitor between the two forms (*19*). The failure of detecting a low-affinity binding state for **1** by the direct binding and inhibition experiments suggests that the two previously observed states of HSPDE4B2B may possess a similar affinity toward binding **1**. To further investigate this, displacement of **1** by (*R*)-

Table 1: Summary of Constants of Inhibition and Binding of Various HSPDE4B2B Deletional Constructs and Site Mutants by **1** Determined at pH 7.0 and 22 °C

HSPDE4B2B	K_d,[a] nM	n[b]	K_i,[a] nM
1−564	2.7 ± 0.7	0.9 ± 0.1	0.54 ± 0.10
81−564	1.9 ± 0.6	1.1 ± 0.2	0.62 ± 0.20
152−528	1.2 ± 0.3	0.9 ± 0.1	0.67 ± 0.13
81−564 SΔA	ND[c]	1.0 ± 0.1	0.46 ± 0.19
152−528 SΔA	ND[c]	0.8 ± 0.1	0.81 ± 0.12

[a] K_d is the dissociation constant from Job plot analysis (eq 24), and K_i is the inhibition constant. The discrepancies between the values of K_i and K_d are ascribed to different systematic errors. [b] The standard error in stoichiometry, n, which was predicted by eq 23, was calculated by using the following error function:

$$\sigma(n) = \frac{1}{i}\sqrt{[\sigma(s_1)]^2 + [\sigma(s_2)]^2 + [\sigma(i_2)]^2\left(\frac{s_1 + s_2}{i_2}\right)^2}$$

[c] Not determined.

rolipram and binding stoichiometry measurements were performed.

*Bound **1** Can Be Fully Displaced by (R)-Rolipram.* In a displacement experiment, [^{3}H]**1** was kept at 2 nM, whereas the concentration of (*R*)-rolipram was varied. If **1** does not bind to one of the two states for (*R*)-rolipram at all, the experiment would show only a single displacement transition and an IC_{50} for (*R*)-rolipram that corresponds to either high- or low-affinity binding. On the other hand, if both the states are occupied by **1**, a double isotherm that resembles the curve for the inhibition of full-length HSPDE4B2B by (*R*)-rolipram (*19*) should be observed (see below). Indeed, as shown in Figure 6A, the two binding affinities for (*R*)-rolipram are both present with the bound **1** being fully displaced. The apparent IC_{50}'s (Table 2), calculated using eq 18, for the high- and low-affinity forms for (*R*)-rolipram from the displacement agree reasonably well with the values (Table 2) determined by independent inhibition and binding studies performed previously (*19*). The data strongly suggest that **1** binds to both states of HSPDE4B2B with high affinity.

*The Stoichiometry of **1** Binding.* If only one of the two states of HSPDE4B2B binds **1**, the stoichiometry of binding would be close to 0.5 since previously the ratio of the two states of HSPDE4B2B was shown to be close to 1:1. On the other hand, the binding of **1** to HSPDE4B2B would show a 1:1 stoichiometry if both states of HSPDE4B2B are accessible by **1** with high affinity. The Job plot method (*21*, *22*) was employed in filter binding assays to determine the stoichiometry. In Job plots the amount of bound species is followed as a function of molar fraction of enzyme at a constant sum of enzyme and ligand. The highest amount of binding occurs at the stoichiometric concentrations of enzyme and ligand (*21*, *22*). As described in Experimental Procedures, the apex value may be evaluated by extrapolating the linear portion of each side of the curve to the intercept of the two lines using the slopes and the *y*-intercept of the line with negative slope (Table 3). As shown in Figure 7A, the peak of the plot corresponds to a molar fraction of ca. 0.53 ± 0.05 (Table 3). Using eq 23, the stoichiometry was calculated to be 0.9 ± 0.1 (Table 1). Assuming a 1:1 molar stoichiometry, a K_d of 2.7 ± 0.7 nM (Table 1) was estimated by fitting data to eq 24. This value is comparable to the values determined by filter binding and inhibition of enzyme activity. These data again support binding of **1** to both states of HSPDE4B2B with high affinity.

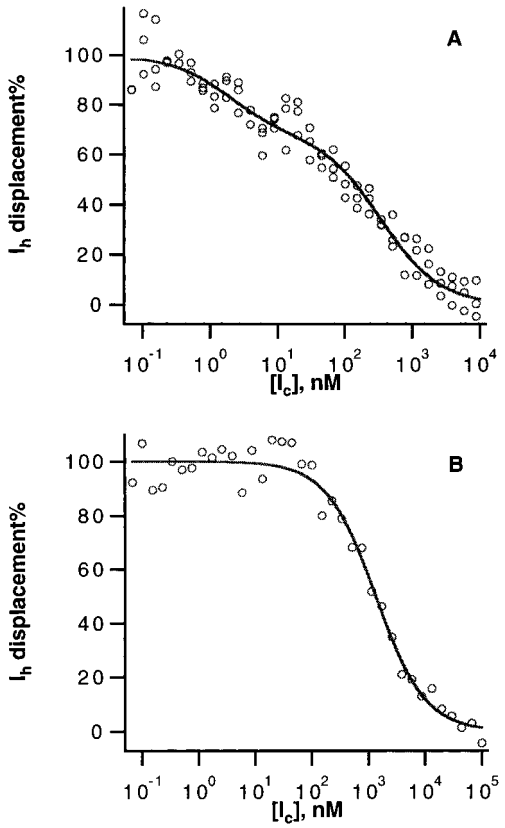

FIGURE 6: Displacement of bound **1** by (*R*)-rolipram using filter binding assays. The concentrations of enzyme and [^{3}H]**1** (I_h) were set to 1 and 2 nM, respectively. [EI_h] at various concentrations of (*R*)-rolipram (I_c) was determined according to the filter binding procedure described in Experimental Procedures. (A) HSPDE4B2B 1−564. Data were fit to eq 18. (B) HSPDE4B2B 152−528. Data were fit to eq 17.

Table 2: Summary of Constants for Displacement of [^{3}H]**1** Bound with HSPDE4B2B by (*R*)-Rolipram

HSPDE4B2B	$(IC_{50})_1$, nM	$(IC_{50})_2$, nM
1−564	340 ± 60 (390 ± 90)[a]	1.8 ± 0.8 (5.6 ± 1.6)[a]
152−528	1400 ± 200	

[a] The values in parentheses were determined by inhibition of HSPDE4B2B by (*R*)-rolipram after a 1-h preincubation of inhibitor with enzyme (*19*).

Table 3: Summary of Job Plot Parameters for Stoichiometry of Binding of **1** to HSPDE4B2B and HSPDE4B2B Truncates

HSPDE4B2B	s_1,[a] nM	s_2,[b] nM	i_2,[c] nM	$(\chi_e)_s$[d]
1−564	94 ± 2	104 ± 6	102 ± 7	0.53 ± 0.05
81−564	103 ± 3	97 ± 7	97 ± 8	0.49 ± 0.05
151−528	95 ± 2	105 ± 4	104 ± 5	0.53 ± 0.03
81−564 SΔA	3881 ± 68	3837 ± 111	3836 ± 52	0.50 ± 0.01
152−528 SΔA	3370 ± 83	2748 ± 211	3339 ± 64	0.55 ± 0.02

[a] The slope from eq 20. [b] The slope from eq 21. [c] The intercept from eq 21. [d] The value of molar fraction of enzyme corresponding to the intercept of eqs 20 and 21 that is given by eq 22. The errors of $(\chi_e)_s$ were calculated by using the error function

$$\sigma((\chi_e)_s) = \frac{1}{s_1 + s_2}\sqrt{[\sigma(i_2)]^2 + \left([\sigma(s_1)]^2 + [\sigma(s_2)]^2\left(\frac{i_2}{s_1 + s_2}\right)^2\right.}$$

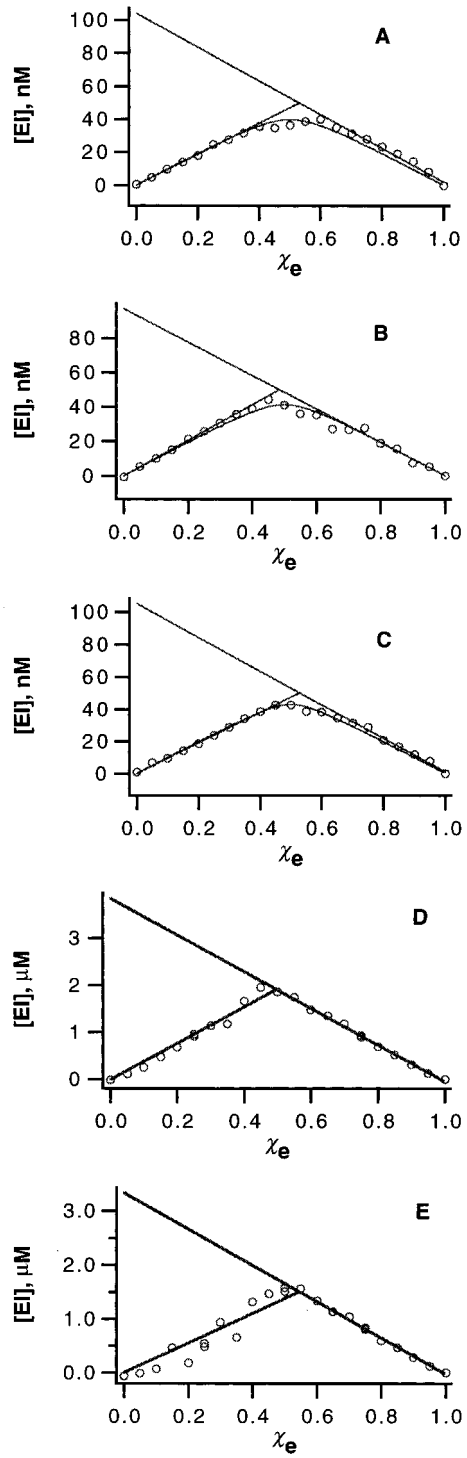

FIGURE 7: Job plot analysis of binding of **1** to HSPDE4B2B mutants by filter binding assays for HSPDE4B2B 1−564 (A), HSPDE4B2B 81−564 (B), and HSPDE4B2B 152−528 (C) and by equilibrium dialysis (see Experimental Procedures) for HSPDE4B2B 81−564 SΔA (D) and HSPDE4B2B 152−528 SΔA (E). The concentration of bound species, [EI], was then plotted against the molar fraction of enzyme, χ_e. The linear solid lines with positive and negative slopes are theoretical values calculated using eqs 20 and 21 for data from 0 to 0.3 and from 0.7 to 1, respectively. The curves in plots A−C are theoretical values calculated using eq 24.

Equilibrium Systems with Multiple States. The presence of two transitions in the displacement experiments described above and in the inhibition and equilibrium binding studies conducted previously (*19*) suggests that the two isostates of HSPDE4B2B are not exchangeable. Theoretical analysis of inhibitor binding in a system of two exchangeable enzyme states, as shown in Scheme 1, and their reduction to nonexchangeable states was performed (Experimental Procedures) to provide further insights. Assuming E_1 and E_2 are exchangeable, the sum of $[E_1I]$ and $[E_2I]$ is given by (sum of eqs 9 and 12)

$$[E_1I] + [E_2I] = E_t\left(\frac{A_1}{(K_{d1})_{app} + [I]} + \frac{A_2}{(K_{d2})_{app} + [I]}\right)[I] \quad (25)$$

According to eqs 10 and 13, $A_1 + A_2 = 1$, and from eqs 3−6, 11, and 14, $(K_{d1})_{app} = (K_{d2})_{app}$; therefore, eq 25 can be expressed as

$$[E_1I] + [E_2I] = E_t\frac{[I]}{(K_d)_{app} + [I]} \quad (26)$$

where

$$(K_d)_{app} = (K_{d1})_{app} = (K_{d2})_{app} \quad (27)$$

Equation 26 predicts a dose−response curve with a monotonic transition that is characteristic of the apparent dissociation constant $(K_d)_{app}$. The value of $(K_d)_{app}$ falls between K_{d1} and K_{d2}, and depending upon the relative values of K_E and K_{EI}, it may resemble K_{d1} or K_{d2}. For nonexchangeable systems (eqs 15 and 16), the sum of $[E_1I]$ and $[E_2I]$ is given by

$$[E_1I] + [E_2I] = \frac{E_{1t}[I]}{K_{d1} + [I]} + \frac{E_{2t}[I]}{K_{d2} + [I]} \quad (28)$$

Equation 28 describes a biphasic transition that is characteristic of K_{d1} and K_{d2} if the values of K_{d1} and K_{d2} are significantly different. This forms the basis for treating the data from the displacement experiments using eq 18 as described in Experimental Procedures.

For inhibition studies, the initial rate under the k_{cat}/K_m condition is given by

$$v = \left(\frac{k_{cat}}{K_m}\right)_1[E_1][S] + \left(\frac{k_{cat}}{K_m}\right)_2[E_2][S] \quad (29)$$

If the system is nonexchangeable, eq 29 can be expressed, using eqs 3, 4, 15, and 16, as

$$v = \left(\frac{k_{cat}}{K_m}\right)_1\frac{E_{1t}[S]}{1 + [I]/K_{d1}} + \left(\frac{k_{cat}}{K_m}\right)_2\frac{E_{2t}[S]}{1 + [I]/K_{d2}} \quad (30)$$

Equation 30 describes a biphasic function. If the system is exchangeable, eq 29 can be expressed, using eqs 5 and 26, as

$$v = \frac{1}{1 + K_E}\left(\left(\frac{k_{cat}}{K_m}\right)_1 K_E + \left(\frac{k_{cat}}{K_m}\right)_2\right)\frac{E_t[S]}{1 + [I]/(K_d)_{app}} \quad (31)$$

Equation 31 predicts a single transition in the initial rate.

*Effect of Deletional Mutations on Properties of Inhibition and Binding of HSPDE4B2B by **1***. HSPDE4B2B retains enzyme activity after the first 151 and the last 36 amino acid residues are truncated from the protein (152−528 construct) (*19*). This truncate, however, appears to only possess the

low-affinity form of HSPDE4B2B in binding (*R*)-rolipram (*19*). Truncation of the first 80 amino acid residues (81−564 construct) did not eliminate the high-affinity binding (*19*). Here, studies were performed to determine if the binding and inhibition of HSPDE4B2B by **1** can be affected by the truncations. Shown in panels B and C of Figure 5 are data of inhibition of HSPDE4B2B 81−564 and 152−528 by **1**, respectively. The inhibitions show only a single transition with a $K_i \sim 1$ nM (Table 1). The stoichiometries (Table 1) were derived from filter Job plots (Figure 7B,C), and the K_d's were obtained using eq 24 (Table 1). These data resemble those of the wild-type 1−564 protein (Table 1). Additionally, **1** bound to HSPDE4B2B 152−528 is fully displaced by (*R*)-rolipram, but the displacement shows only a single transition (Figure 6B). These data indicate high-affinity binding and inhibition, by **1**, of the HSPDE4B2B form that binds (*R*)-rolipram with low affinity.

*Effect of Site-Directed Mutations on Inhibition and Binding of HSPDE4B2B by **1**.* Purified full-length HSPDE4B2B or HSPDE4B2B 81−564 construct contains either monophosphorylation at serine 487 or diphosphorylation at serines 487 and 489. Recent data (*19*) indicated that (*R*)-rolipram binding and inhibition of HSPDE4B2B as well as the ratio of the two states of the enzyme were not dramatically affected by mutations of these serine residues. We determined if phosphorylation had any effect on the properties of inhibition and binding of HSPDE4B2B by **1**. Panels D and E of Figure 5 show the results of inhibition of HSPDE4B2B 81−564 SΔA and HSPDE4B2B 152−528 SΔA, respectively, and the K_i values are listed in Table 1. The data indicate that the mutations had little effect on the inhibition of HSPDE4B2B by **1**. The fact that binding stoichiometries, as shown in panels D and E of Figure 7 by equilibrium dialysis Job plot assays, are close to 1:1 for both HSPDE4B2B 81−564 SΔA and 152−528 SΔA mutants (Table 1) rules out the presence of a state in HSPDE4B2B 81−564 SΔA that is not inhibited by **1**.

DISCUSSION

Contrary to early reports of a catalytically inactive high-affinity binding site for (*R*)-rolipram and a catalytically active low-affinity site for the same inhibitor that coexist on PDE 4 (*16*), recent studies (*19*) demonstrated the presence of two HSPDE4B2B states with both the states being catalytically active, but differing in their affinities for (*R*)-rolipram. The low-affinity state binds (*R*)-rolipram at >200 nM and does so rapidly, whereas the high-affinity state binds (*R*)-rolipram at ca. 1 nM, and this tight binding develops relatively slowly with time. While maintenance of the low-affinity state for (*R*)-rolipram only requires the catalytic domain (152−528), formation of the high-affinity state requires the presence of the N-terminal residues 81−151 and the catalytic domain. Oligomerization does not appear to contribute to (*R*)-rolipram binding to the 152−528 construct, although its role in (*R*)-rolipram binding to the full-length protein has not been ruled out. The role of phosphorylation of the protein in the time-dependent formation of the high affinity state remains unresolved, although if it does play a role, it must do so in the presence of the N-terminal residues. Although the existence of two states in (*R*)-rolipram binding had been demonstrated, whether the accessibility to these states by other inhibitors required further investigation.

In the present study, we examined the interaction of a novel PDE 4 inhibitor, **1** (Figure 1), with HSPDE4B2B using a combination of kinetic, thermodynamic, and molecular biology approaches. The data presented here indicate the capability of **1** to interact with both of the isostates of PDE 4 that were observed in (*R*)-rolipram binding, thereby demonstrating that the presence of isostates in PDE 4 is not a unique phenomenon that is only associated with the (*R*)-rolipram binding. However, **1** is not discriminative in binding and inhibition of the two isostates of HSPDE4B2B as is (*R*)-rolipram. In contrast to displaying different affinities for (*R*)-rolipram, the two HSPDE4B2B isostates bind **1** with a single, high affinity. Given that the K_i values for **1** from inhibition of enzyme activity were obtained within minutes, whereas the K_d values from binding experiments were determined after an hour long preincubation, it is unlikely that a time-dependent component was involved in developing the apparently high binding affinity of HSPDE4B2B for **1** as it was observed for (*R*)-rolipram. The N-terminal residues 81 to 151 have no effect on the binding affinity of HSPDE4B2B for **1** as these residues do in binding (*R*)-rolipram, nor does the phosphorylation state have any effect on the binding and inhibition properties of **1**.

A fundamental question about the two isostate system of HSPDE4B2B is whether the two isostates are physically exchangeable. The observation of two transitions in the equilibrium (*R*)-rolipram binding and inhibition of HSPDE4B2B by (*R*)-rolipram (*19*) and in the displacement of **1** bound to HSPDE4B2B by (*R*)-rolipram performed in this study suggests that the two HSPDE4B2B isostates are nonexchangeable. This is supported by theoretical analysis of a general two isostate system (Scheme 1). As indicated by eq 26 (Results), if the two isostates are exchangeable, only a single, monotonic transition should be observed in equilibrium binding of inhibitor or in equilibrium displacement of a bound inhibitor by another, regardless how far apart the two true K_d values are. The same conclusion can be drawn for inhibition of the two states even if the two states have distinct enzymatic activities (eq 31, Results). If the two isostates are nonexchangeable, two transitions will be observed by both binding (eq 28, Results) and inhibition kinetics (eq 30, Results), provided that the dissociation constants for the two isostates are significantly different.

The nature of the physical barrier to the interconversion between the two isostates of HSPDE4B2B remains an open question. Theoretically, deep wells in the free energy conformational hypersurface of a protein may exist that can trap certain molecular conformers and prevent the kinetic interconversion between these conformers. Hypothetical examples of such conformers may include protein or RNA molecules in which a knot is formed.[2] However, to date there is no evidence supporting the existence of such trapped conformers in HSPDE4B2B, and we consider such scenarios unlikely. The absence of disulfides in HSPDE4B2B (W. J. Rocque, unpublished data) rules out distinct, stable, three-dimensional structures arising from swapping between disulfides. Since the presence of the two isostates requires the presence of the N-terminal residues 81−151 of HSPDE4B2B, the formation of nonexchangeable states cannot be ascribed

[2] As pointed out by one referee, stable protein conformers may also arise from the action of certain chaperonins.

Scheme 2: Kinetic and Thermodynamic Models for (*R*)-Rolipram Binding to HSPDE4B2B[a]

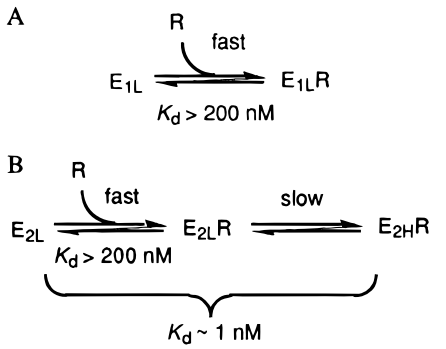

[a] (A) Binding of R to the low-affinity state, E_{1L}, of HSPDE4B2B. (B) Binding of R to E_{2L}, the low-affinity precursor to the high-affinity state, E_{2H}, of HSPDE4B2B and the time-dependent conversion of $E_{2L}R$ to $E_{2H}R$.

to the presence of potential stable conformers of inhibitor. It is conceivable that structural differences due to changes in the primary sequence may account for the presence of nonexchangeable species. The recombinant HSPDE4B2B purified from baculovirus expression was heterogeneously phosphorylated at serines 487 and 489, and the ratio for the unphosphorylated and the phosphorylated species was about 1:1 (*17*), resembling that (1:1) for the two isostates. The biological relevance of the phosphorylation of PDE 4 is not clear, although this phosphorylation can be accomplished by MAPK in vitro (*17*). However, as pointed out by Rocque et al. (*19*), the phosphorylation state does not appear to be responsible for the observed high affinity for (*R*)-rolipram binding to HSPDE4B2B, because 81−564 SΔA, which is not phosphorylated, still retains the high-affinity (*R*)-rolipram binding.

To better understand the results between (*R*)-rolipram and **1**, we constructed kinetic and thermodynamic models that can accommodate the data on inhibition and binding of HSPDE4B2B. Since the high-affinity state of HSPDE4B2B for (*R*)-rolipram develops only after a period of time upon addition of (*R*)-rolipram (*19*), HSPDE4B2B must exist in two low-affinity states prior to the binding by (*R*)-rolipram. Here, these two low-affinity states for (*R*)-rolipram are designated E_{1L} and E_{2L} (Scheme 2A), with the latter referring to the low-affinity precursor to the high-affinity state, E_{2H}. As depicted by Scheme 2A, the equilibrium for binding of (*R*)-rolipram, hereafter abbreviated as R, to the E_{1L} state is fast, forming an $E_{1L}R$ complex with a $K_d > 200$ nM. The binding reaction between (*R*)-rolipram and E_2 is more complicated due to the time-dependent nature of this binding (*19*). Here we propose a two-step mechanism for this binding (Scheme 2B). The first step is fast, forming a loosely bound $E_{2L}R$ complex. This step is followed by a slow reorganization within the loose complex that ultimately leads to a tight-binding complex, $E_{2H}R$. This two-step mechanism is consistent with the observation of an initial inhibition of HSPDE4B2B by (*R*)-rolipram, with a $K_d > 200$ nM, that precedes a time-dependent onset of a more potent inhibition with an overall $K_d \sim 1$ nM (*19*). The precise kinetic and thermodynamic properties associated with this process require further studies. The mechanism for binding of **1** to HSPDE4B2B appears simpler. Compound **1** binds to E_{1L} or E_{2L} with a K_d of ~1 nM in a single, fast step as shown in parts A and B, respectively, of Scheme 3. However, it cannot be ruled out that binding of **1** to E_{2L} may also involve two steps, as does binding of (*R*)-rolipram, and that both steps are fast, leading to a final complex of E_{2H}**1** without displaying time dependence. These alternative mechanisms await further investigation.

Scheme 3: Kinetic and Thermodynamic Models for Binding of **1** to HSPDE4B2B[a]

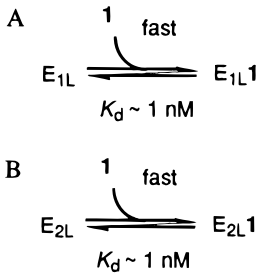

[a] (A) Binding of **1** to E_{1L} of HSPDE4B2B. (B) Binding of **1** to E_{2L} of HSPDE4B2B.

Generally, time-dependent inhibition can be reversible or irreversible and may be caused by chemical transformations or slow conformational changes in enzyme (*22*). Given the apparent lack of chemically reactive centers in (*R*)-rolipram, it is unlikely that the time-dependent inhibition of E_2 by (*R*)-rolipram is caused by chemical modification of HSPDE4B2B by the inhibitor. It is more probable that the time dependence is caused by a conformational change in E_2 of HSPDE4B2B upon (*R*)-rolipram binding. Since the N-terminal residues 81−151 are necessary for expressing the high-affinity state for (*R*)-rolipram, conformational changes involving these residues may be responsible for the observed time dependence. HSPDE4B2B is known to oligomerize at micromolar concentrations (*18*). Addition of (*R*)-rolipram to HSPDE4B2B at micromolar concentrations does not appear to alter the protein oligomerization states as revealed by light scattering techniques (*18*). However, it cannot be ruled out that (*R*)-rolipram binding may perturb the oligomerization states of HSPDE4B2B under catalytic conditions and that this perturbation may play a role in the observed time-dependent inhibition. It is puzzling that **1** does not induce time-dependence in its binding to HSPDE4B2B as does (*R*)-rolipram. In the absence of the three-dimensional structure of the protein−inhibitor complex, the nature of the conformation-based time dependence in the inhibition of HSPDE4B2B by (*R*)-rolipram will remain unresolved.

It is interesting that the isostates of PDE 4 described by in vitro experiments were also observed in vivo with different tissue distributions. For example, high affinity binding and low-affinity inhibition of PDE 4 by (*R*)-rolipram were found in brain and airway smooth muscles, whereas in many peripheral tissues, only the low affinity form was detected (*13*, *16*). The variable distribution of E_1 and E_2 of PDE 4 in vivo suggests that these states may have different biological functions. Since PDE 4 has been implicated in a number of diseases, such as asthma and depression, state-specific inhibitors of type 4 PDE may have different therapeutic benefits. Given that it is a poor inhibitor of the E_1 state, (*R*)-rolipram may be considered as being only specific for the E_2 state. Now **1**, a novel PDE 4 inhibitor, has been demonstrated to be equally potent for inhibition or binding of both E_1 and E_2, adding a dual inhibitor of the

HSPDE4B2B isostates. It remains to be seen if inhibitors that are only specific for E_1 can be identified.

APPENDIX A: DERIVATION OF EQUATIONS 9 AND 12 IN THE TEXT

For a two enzyme state system as shown by Scheme 1, the following set of linear, independent equations can be derived using eqs 3−7 in the text:

$$\frac{1 + K_{EI}}{K_{EI}}[E_1I] + (1 + K_E)[E_2] = E_t \quad \text{(A1)}$$

$$(1 + K_{EI})[E_2I] + (1 + K_E)[E_2] = E_t \quad \text{(A2)}$$

and

$$[E_2I] + \left(1 + K_E + \frac{[I]}{K_{d1}}\right)[E_2] = E_t \quad \text{(A3)}$$

Solving for $[E_1I]$ and $[E_2I]$, we have

$$[E_1I] = \frac{\frac{K_{EI}}{1 + K_{EI}}[I]}{K_{EI}\frac{1 + K_E}{1 + K_{EI}}K_{d1} + [I]}E_t \quad \text{(A4)}$$

and

$$[E_2I] = \frac{\frac{1}{1 + K_{EI}}[I]}{K_{EI}\frac{1 + K_E}{1 + K_{EI}}K_{d1} + [I]}E_t \quad \text{(A5)}$$

Equation A4 is identical to eq 9 in the text. Obeying the principle of microscopic reversibility, the ratio K_{d1}/K_{d2} is given by

$$\frac{K_{d1}}{K_{d2}} = \frac{K_E}{K_{EI}} \quad \text{(A6)}$$

Solving eq A6 for K_{d1} and substituting the K_{d1} in eq A5, we arrive at

$$[E_2I] = \frac{\frac{1}{1 + K_{EI}}[I]}{K_E\frac{1 + K_E}{1 + K_{EI}}K_{d2} + [I]}E_t \quad \text{(A5)}$$

which is equivalent to eq 12 in the text.

APPENDIX B: DERIVATION OF EQUATION 24 IN THE TEXT

For an equilibrium of binding between enzyme and inhibitor, the concentration of EI complex, [EI], can be calculated by

$$[EI] = {}^1/_2(E_t + I_t + K_d - \sqrt{(E_t + I_t + K_d)^2 - 4E_tI_t}) \quad \text{(B1)}$$

where E_t and I_t are total concentration of enzyme and inhibitor, respectively, and K_d is the dissociation constant. In Job plot,

$$E_t + I_t = C_t \quad \text{(B2)}$$

E_t is given by

$$E_t = C_t\chi_e \quad \text{(B3)}$$

where χ_e is the molar faction of enzyme. Accordingly, I_t may be expressed as

$$I_t = C_t(1 - \chi_e) \quad \text{(B4)}$$

Bringing eqs B2, B3, and B4 into eq B1, we arrive at eq 24 in the text:

$$[EI] = {}^1/_2(C_t + K_d - \sqrt{(C_t + K_d)^2 - 4C_t{}^2(\chi_e - \chi_e{}^2)}) \quad \text{(B5)}$$

REFERENCES

1. Beavo, J. A. (1988) in *Advances in Second Messenger and Phosphoprotein Research* (Greengard, P., and Robison, G. A., Eds.) Vol. 22, pp 1−38, Raven Press, New York.
2. Beavo, J. A., and Reifsnyder, D. H. (1990) *Trends Pharmacol. Sci. 11*, 150−155.
3. Michaeli, T., Bloom, T. J., Martins, T., Loughney, K., Ferguson, K., Riggs, M., Rodgers, L., Beavo, J. A., and Wigler, M. (1993) *J. Biol. Chem. 268*, 12925−12932.
4. Farber, D. B., Bowes, C., and Danciger, M. (1991) *Prog. Clin. Biol. Res. 362*, 67−89.
5. Pittler, S. J., and Baehr, W. (1991) *Proc. Natl. Acad. Sci. U.S.A. 88*, 8322−8326.
6. Lee, H. R., Hershberger, R. E., Port, J. D., Rasmussen, R., Renlund, D. G., O'Connell, J. B., Gilbert, E. M., Mealey, P. C., Volkman, K., and Menlove, R. (1991) *J. Thorac. Cardiovasc. Surg. 102*, 246−258.
7. O'Connell, J. B., Gilbert, E. M., Renlund, D. G., and Bristow, M. R. (1991) *J. Heart Lung Transplant. 10*, 477−481.
8. Torphy, T. J. (1988) *Agents Actions 23* (Suppl), S37−53.
9. Torphy, T. J., and Hay, D. W. P. (1990) in *Airway smooth muscle: modulation of receptors and response* (Townley, R. G., and Agrawal, D. K., Eds.) pp 39−68, CRC Press, Boca Raton.
10. Bourne, H. R., Lichtenstein, L. M., Melmon, K. L., Henney, C. S., Weinstein, Y., and Shearer, G. M. (1974) *Science 184*, 19−28.
11. Plaut, M., Marone, G., Thomas, L. L., and Lichtenstein, L. M. (1980) *Adv. Cyclic Nucleotide Res. 12*, 161−172.
12. Kaehl, F. A., Zannetti, M. E., Soderman, D. D., Miller, K. D., and Ham, E. A. (1987) *Am. Rev. Respir. Dis. 136*, 210−213.
13. Schneider, H. H., Schmiechen, R., Brezinski, M., and Seidler, J. (1986) *Eur. J. Pharmacol. 127*, 105−115.
14. Saccomano, N. A., Vinick, F. J., Koe, B. K., Nielsen, J. A., Whalen, W. M., Moletz, M., Philips, D., Thadieo, P. F., Jung, S., Chapin, D. S., Lebel, L. A., Russo, L. L., Heleveg, D. A., Johnson, J. L., Ives, J. F., and Williams, I. H. (1991) *J. Med. Chem. 34*, 291−298.
15. Nemoz, G., Moueqqit, M., Prigent, A.-F., and Pacheco, H. (1989) *Eur. J. Biochem. 184*, 511−520.
16. Torphy, T. J., Stadel, J. M., Burman, M., Cieslinski, L. B., McLaughlin, M. M., White, J. R., and Livi, G. P. (1992) *J. Biol. Chem. 267*, 1798−1804.
17. Lenhard, J. M., Kassel, D. B., Rocque, W. J., Hamacher, L., Holmes, W. D., Patel, I., Hoffman, C., and Luther, M. A. (1996) *Biochem. J. 316*, 751−758.
18. Rocque, W. J., Holmes, W. D., Patel, I. R., Dougherty, R. W., Ittoop, O., Overton, L., Hoffman, C. R., Wisely, G. B., Willard, D. H., and Luther, M. A. (1997) *Protein Expression Purif. 9*, 191−202.

19. Rocque, W. J., Tian, G., Wiseman, J. S., Holmes, W. D., Thompson, I. Z., Willard, D. H., Patel, I. R., Wisely, G. B., Clay, W. C., Kadwell, S. H., Hoffman, C. R., and Luther, M. A. (1997) *Biochemistry 36*, 14250−14261.
20. Stafford, J. A., Veal, J. M., Feldman, P. L., Valvano, N. L., Baer, P. G., Brackeen, M. F., Brawley, E. S., Connolly, K. M., Domanico, P. L., Han, B., Rose, D. A., Rutkowske, R. D., Sekut, L., Stimpson, S. A., Strickland, A. B., and Verghese, M. W. (1995) *J. Med. Chem. 38*, 4972−4975.
21. Felsenfeld, G., and Miles, H. T. (1957) *Annu. Rev. Biochem. 36*, 407−649.
22. Cantor, C. R., and Schimmel, P. R. (1980) *Biophysical Chemistry Part III: The Behavior of Biological Macromolecules*, W. H. Freeman and Co., New York.
23. Morrison, J. F., and Walsh, C. T. (1988) *Adv. Enzymol. Relat. Areas Mol. Biol. 61*, 201−301.

BI972700V